Available online at www.sciencedirect.com
SCIENCE DIRECT®
Advances in Space Research 37 (2006) 1287–1291
ADVANCES IN SPACE RESEARCH
(a COSPAR publication)
www.elsevier.com/locate/asr

The role of Hall currents on incompressible magnetic reconnection

Laura F. Morales [a,*], Sergio Dasso [b,c], Daniel O. Gómez [b,c], Pablo D. Mininni [c,1]

[a] Département de Physique, Université de Montréal, C.P. 6128, succ. Centre-ville, Montréal, Que., Canada H3C 3J7
[b] Instituto de Astronomía y Física del Espacio, CC. 67, suc. 28, 1428 Buenos Aires, Argentina
[c] Departamento de Física, Facultad de Ciencias Exactas y Naturales, Universidad de Buenos Aires, 1428 Buenos Aires, Argentina

Received 13 October 2004; received in revised form 28 June 2005; accepted 29 June 2005

Abstract

Magnetic reconnection is one of the most important energy conversion processes in space plasmas. Theoretical models of magnetic reconnection have been traditionally developed within the framework of magnetohydrodynamics (MHD). However, in low density astrophysical plasmas as those found in the magnetopause and the magnetotail, the current sheet thickness can be comparable to the ion inertial scale and therefore the Hall electric field becomes non-negligible. The role of the Hall current is to increase the reconnection rate with respect to MHD predictions, which therefore poses a promising mechanism for fast reconnection. We present results from parallel simulations of the incompressible Hall MHD equations in $2\frac{1}{2}$ dimensions. We quantitatively evaluate the relevance of the Hall current in the reconnection process by performing a set of simulations with different values of the Hall parameter. We compute the corresponding reconnection rates as a function of time, and explore the spatial structure of the fields in the surroundings of the diffusion region. We quantify the increase of the reconnection rate as a function of the Hall parameter, and confirm the presence of a quadrupolar structure for the out-of-plane magnetic field.
© 2006 Published by Elsevier Ltd on behalf of COSPAR.

Keywords: Magnetic reconnection; Hall current; Solar wind and magnetosphere

1. Introduction

Magnetic reconnection is likely to be the main mechanism by which the energy stored in stressed magnetic fields can be converted into kinetic and thermal energy. It is believed to play a crucial role in different astrophysical environments such as the Earth's magnetopause Sonnerup et al. (1981), the Earth's magnetotail (here it is related to the release of magnetic energy, see e.g., Birn and Hesse (1996)), the solar atmosphere (related to the occurrence of flares, coronal mass ejections, and coronal heating, see e.g. Priest (1984), Gosling et al. (1995)), or the interplanetary medium (for instance, as a consequence of the interaction between magnetic clouds and the solar wind, see Farrugia et al. (2001), Schmidt and Cargill (2003)).

Hall currents can in turn play a significant role in the dynamics of low density and/or low temperature astrophysical plasmas, for which a one fluid description has been traditionally used. For instance, they can alter the dynamics of magnetic fields in dense molecular clouds, trigger instabilities in accretion disks or modify the efficiency of turbulent dynamos (Minnini et al., 2003). Due to the low density of the plasma in the solar wind and magnetosphere, the Hall currents can also be of importance during magnetic reconnection at the Earth's magnetopause, and some signatures of these Hall currents have been reported (Mozer et al., 2002). However, the quantitative importance of its contribution to magnetic reconnection is still being assessed in

* Corresponding author. Tel.: +1 514 343 6111/3698; fax: +1 514 343 2071.
E-mail address: laura@astro.umontreal.ca (L.F. Morales).
[1] Present address: Advanced Study Program (NCAR), P.O. Box 3000, Boulder, CO 80307, USA.

0273-1177/$30 © 2006 Published by Elsevier Ltd on behalf of COSPAR.
doi:10.1016/j.asr.2005.06.054

the literature (see for example: Craig et al. (2003) and Birn et al. (2001) and references therein).

Theoretical models of magnetic reconnection have been traditionally developed within the framework of magnetohydrodynamics (notably Parker (1957) and Petschek (1964)). Nevertheles, in recent years many analytical and computational efforts have been made to clarify the importance of the Hall effect in the reconnection process (Craig and Watson, 2003; Smith et al., 2004; Chacón et al., 2003; Dorelli and Birn, 2003; Dorelli, 2003).

In this paper, we study the importance of the Hall term in incompressible magnetic reconnection. We perform numerical simulations of an incompressible $2\frac{1}{2}$D Hall MHD code with different values of the dimensionless parameter ϵ, which measures the relative importance of the Hall current.

In Section 2, we introduce the Hall MHD equations as well as the $2\frac{1}{2}$D configuration. The basis of the numerical model, boundary and initial conditions are presented in Section 3. Section 4 is devoted to the analysis of the role played by the Hall currents and Section 5 contains the summary of the results presented in this paper.

2. Hall MHD model

Highly conductive plasmas (i.e., $S \gg 1$) tend to develop thin and intense current sheets in their reconnection layers. Whenever the current width reaches values as low as c/w_{pi} (w_{pi} is the ion plasma frequency and c is the speed of light), the standard Ohm's law needs to be extended, since it is not possible to neglect the Hall term (Ma and Bhattacharjee, 2001). For a fully ionized plasma of protons and electrons, the generalized Ohm's law can be written as:

$$\boldsymbol{E} + \frac{1}{c}\boldsymbol{v} \times \boldsymbol{B} = \frac{1}{\sigma}\boldsymbol{j} + \frac{1}{ne}\left(\frac{1}{c}\boldsymbol{j} \times \boldsymbol{B} - \nabla p_{\mathrm{e}}\right), \tag{1}$$

where n is the electron and proton density (under the quasi-neutrality hypothesis), e is the charge of the electron, σ is the electric conductivity, $\boldsymbol{v}$ is the plasma flow velocity, and $\boldsymbol{j}$ is the electric current density. Assuming incompressibility (i.e., $\nabla \cdot \boldsymbol{v} = 0$), the so-called Hall-MHD equations can be cast in their dimensionless form as:

$$\partial_t \boldsymbol{v} + (\boldsymbol{v} \cdot \nabla)\boldsymbol{v} = (\nabla \times \boldsymbol{B}) \times \boldsymbol{B} - \nabla p + \nu \nabla^2 \boldsymbol{v}, \tag{2}$$

$$\partial_t \boldsymbol{B} = \nabla \times [(\boldsymbol{v} - \epsilon \nabla \times \boldsymbol{B}) \times \boldsymbol{B}] + \eta \nabla^2 \boldsymbol{B}, \tag{3}$$

$$\nabla \cdot \boldsymbol{B} = 0 = \nabla \cdot \boldsymbol{U}. \tag{4}$$

In Eqs. (2)–(4), we have normalized $\boldsymbol{B}$ and $\boldsymbol{v}$ to the Alfvén speed $v_{\mathrm{a}} = B_0/\sqrt{4\pi\rho}$ (where B_0 is a typical magnetic field intensity and ρ is the mass density), the total gas pressure p to ρv_{a}^2, and longitudes and times, respectively, to L_0 and L_0/v_{a}. The dimensionless dissipation coefficients are the viscosity ν and the electric resistivity η defined as

$$\eta = \frac{c^2}{4\pi\sigma}. \tag{5}$$

The dimensionless coefficient ϵ is defined as

$$\epsilon = \frac{c}{w_{\mathrm{pi}} L_0}, \tag{6}$$

is a measure of the relative strength of the Hall effect. The dimensionless electron velocity is

$$\boldsymbol{v}_{\mathrm{e}} = \boldsymbol{v} - \epsilon \nabla \times \boldsymbol{B}. \tag{7}$$

From Eq. (3) it is apparent that in the non-dissipative limit (i.e., $\eta \to 0$) the magnetic field remains frozen to the electron flow $\boldsymbol{v}_{\mathrm{e}}$ rather than to the bulk velocity $\boldsymbol{v}$.

The incompressible Hall MHD simulations reported in this paper are carried out under the geometric approximation known as $2\frac{1}{2}$D (two and a half dimensions).

This approximation is based on the assumption that there is translational symmetry along the $\hat{z}$ coordinate (i.e., $\partial_z = 0$). Therefore, the solenoidal magnetic and velocity fields, can be represented as:

$$\boldsymbol{B} = \nabla \times [\hat{z} a(x, y, t)] + \hat{z} b(x, y, t), \tag{8}$$

$$\boldsymbol{U} = \nabla \times [\hat{z} \phi(x, y, t)] + \hat{z} u(x, y, t), \tag{9}$$

where $a(x, y, t)$ is the magnetic flux function and $\phi(x, y, t)$ is the stream function. In this approximation, the Hall MHD equations take the form:

$$\partial_t a = [\phi - \epsilon b, a] + \eta \nabla^2 a, \tag{10}$$

$$\partial_t b = [\phi, b] + [u - \epsilon j, a] + \eta \nabla^2 b, \tag{11}$$

$$\partial_t w = [\phi, w] + [j, a] + \nu \nabla^2 w, \tag{12}$$

$$\partial_t u = [b, a] + [\phi, u] + \nu \nabla^2 u. \tag{13}$$

The nonlinear terms are the standard Poisson brackets (i.e., $[p, q] = \partial_x p \partial_y q - \partial_y p \partial_x q$), $w = -\nabla^2 \phi$ is the $\hat{z}$-component of the flow vorticity and $j = -\nabla^2 a$ is the $\hat{z}$-component of the electric current density which vectorial expression can be written:

$$\boldsymbol{j} = \nabla \times b\hat{z} + j\hat{z}. \tag{14}$$

The set of Eqs. (10)–(13) completely describes the reconnection problem for this particular geometry. One of the most important consequences of including the Hall effect is the coupling between the $\hat{z}$-component of the fields to the scalar potentials a and ϕ. Note that if $\epsilon = 0$, then the system decouples and the solutions for a and ϕ are determined by the solution of Eqs. (10) and (12), thus becoming completely independent from the $\hat{z}$ fields.

3. Simulation model

In the present paper, we study the Hall reconnection phenomena by means of the numerical integration of

Eqs. (10)–(13). The computation is carried out in a rectangular domain assuming periodic boundary conditions. The spatial coordinates span the ranges $-\pi \leqslant x, y \leqslant \pi$. The magnetic vector potential $a(x, y, t)$, the stream function $\phi(x, y, t)$ and $\hat{z}$-components of the magnetic field $b(x, y, t)$ and velocity field $u(x, y, t)$ are expanded in their corresponding spatial Fourier amplitudes $a_{\boldsymbol{k}}(t)$, $\phi_{\boldsymbol{k}}(t)$, $b_{\boldsymbol{k}}(t)$ and $u_{\boldsymbol{k}}(t)$. The equations for these Fourier amplitudes are evolved in time using a second order Runge-Kutta scheme and the nonlinear terms are evaluated following a 2/3 dealiased pseudospectral technique. In order to provide a reconnection scenario, the present simulations start with the fluid at rest, and the following initial condition for the $\hat{x}$ component of the magnetic field:

$$\boldsymbol{B}_y(x, y, t) = \begin{cases} B_0 \tanh[\frac{x-\pi/2}{\Delta}] & \text{if } -\pi \leqslant y < 0, \\ -B_0 \tanh[\frac{x+\pi/2}{\Delta}] & \text{if } 0 \leqslant y < \pi. \end{cases} \quad (15)$$

corresponding to a periodic array of oppositely oriented current sheets. In the present paper, we chose $B_0 = 1$ and $\Delta = 0.04\pi$, to simulate two initially thin current sheets, where the reconnection process will take place. In order to drive reconnection, a monocromatic perturbation with $k_x = 1$ and an amplitude of 2% of the initial magnetic profile (see Eq. (15)) is added to the initial condition in the full rectangular domain.

We performed numerical simulations with a moderate spatial resolution of 256×256 grid points, and different values of the Hall parameter ($\epsilon = 0.00$, 0.07, 0.15), to study the role of the Hall term in the overall dynamics of the reconnection process. We also run a set of low-resolution simulations (128×128 grid points) for several values of ϵ ($\epsilon = 0.00$, 0.01, 0.03, 0.06, 0.10, 0.15), to compute the total reconnected flux. In all these simulations, the dissipation coefficients are set to $\eta = \nu = 0.01$ to ensure that all the lengthscales are properly resolved. Note that pseudospectral methods conserve the energy of the system, i.e., no numerical dissipation is artificially introduced by the simulation (Canuto et al., 1988).

4. Hall effect and reconnection

Fig. 1 shows the behavior of the potentials a and ϕ for the case $\epsilon = 0$, i.e., for a purely MHD simulation. The initial magnetic field given by Eq. (15) relaxes to this configuration with an X-point centered at $x = \pi/2, y = 0$ and another one at $x = -\pi/2, y = \pi$ (see Fig. 1(a)). The velocity field displays the typical quadrupolar structure around X-points. The $\hat{z}$ components of the magnetic (i.e., b) and velocity (i.e., u) fields are initially zero, and remain equal to zero for $\epsilon = 0$ (see Eqs. (11) and (13)).

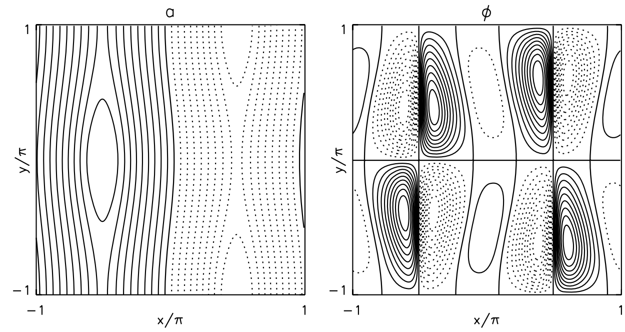

Fig. 1. Contour labels of potentials $a(x, y)$ and $\phi(x, y)$ at $t = 2$, for a purely MHD simulation (i.e., $\epsilon = 0$) with 256^2 grid points. The continuous traces correspond to positive levels, and the dotted traces to negative labels.

When $\epsilon \neq 0$, the configuration of potentials a and ϕ changes, but not in any essential manner, as shown in the two upper panels of Fig. 2. The $\hat{z}$ components of the fields, on the other hand, acquire a sizeable fraction of the total energy. As shown by the lower panels of Fig. 2, the out-of-plane magnetic field component develops a quadrupolar structure around the X-points, as reported by previous authors (Sonnerup, 1979; Terasawa, 1984). This component of the magnetic field is produced by the difference between the ion and electron flows in the reconnection region which leads to the appearence of in-plane Hall currents. Fig. 2 also shows the development of out-of-plane flows in the surroundings of the current layers.

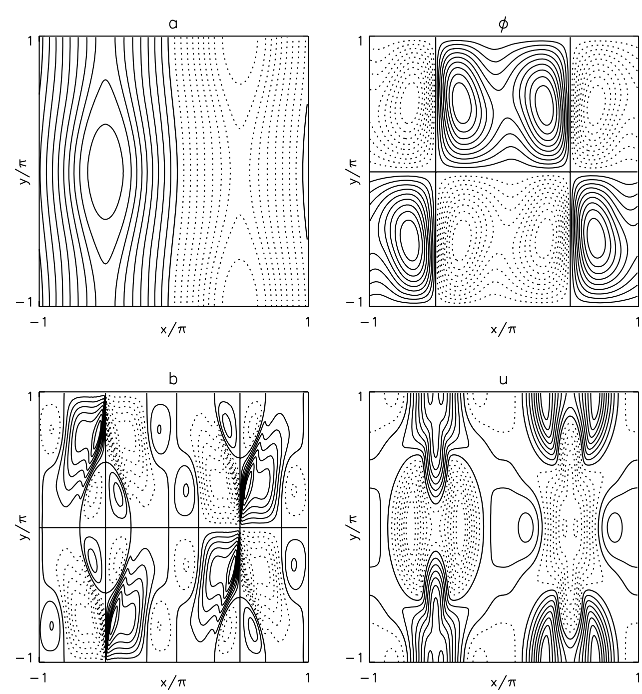

Fig. 2. Contour labels of potentials $a(x, y)$ and $\phi(x, y)$ at $t = 2$ (upper panels) and the z-components of the magnetic (b) and velocity (u) fields (lower panels). It corresponds to a Hall MHD simulation with $\epsilon = 0.07$, and 256^2 grid points. The continuous traces correspond to positive levels, and the dotted traces to negative labels.

The upper panel of Fig. 3 presents the spatial distribution of the out-of-plane electric current density for the case with no Hall effect. Two relatively thin current sheets with opposite orientations can be observed at the sites indicated by the X-points in Fig. 1. In the lower panel of Fig. 3, we show the resulting current distribution for the case where the Hall parameter is $\epsilon = 0.07$. It can be readily seen that the current sheet becomes shorter and thinner and resembles a structure of the type suggested by Petschek. This shortening and shrinking of the current sheet comes along with the appearance of a complex structure for the $\hat{z}$-components of the magnetic field and the velocity, as already shown in the lower panels of Fig. 2. These intense current layers coming out from the X-points coincide with the location of separatrices of the out-of-plane magnetic field (see Fig. 2).

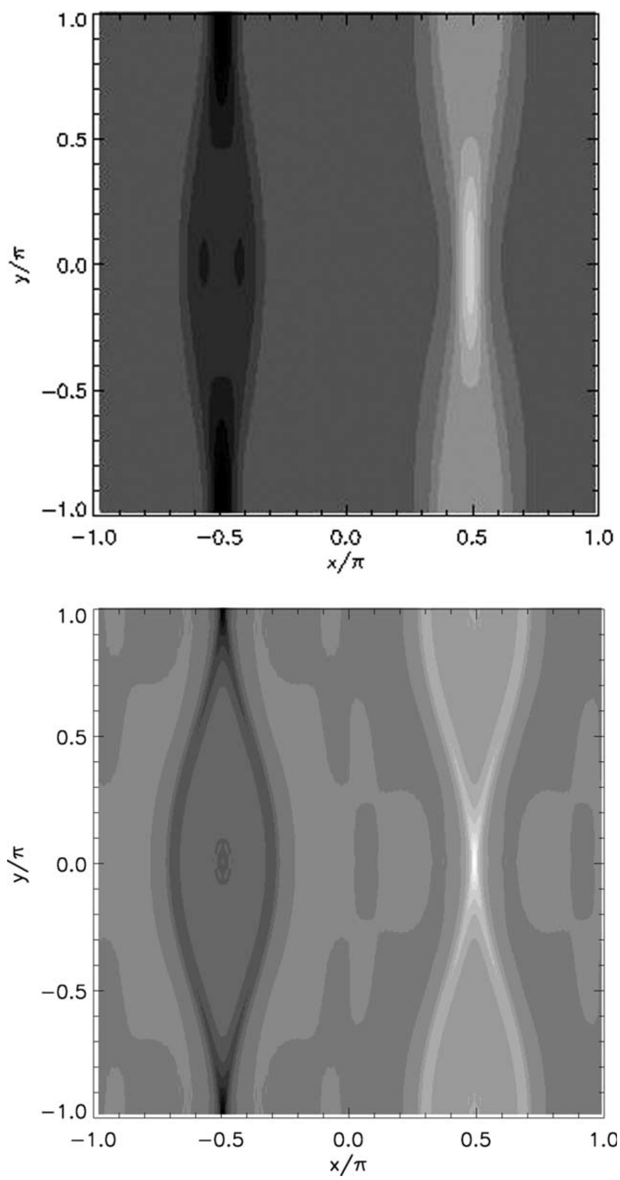

Fig. 3. Halftones of the electric current density component along the z-direction, $j(x, y)$ for simulations of 256^2 grid points, taken at $t = 2$. The upper panel corresponds to $\epsilon = 0$ (i.e., purely MHD) and the lower panel to $\epsilon = 0.07$.

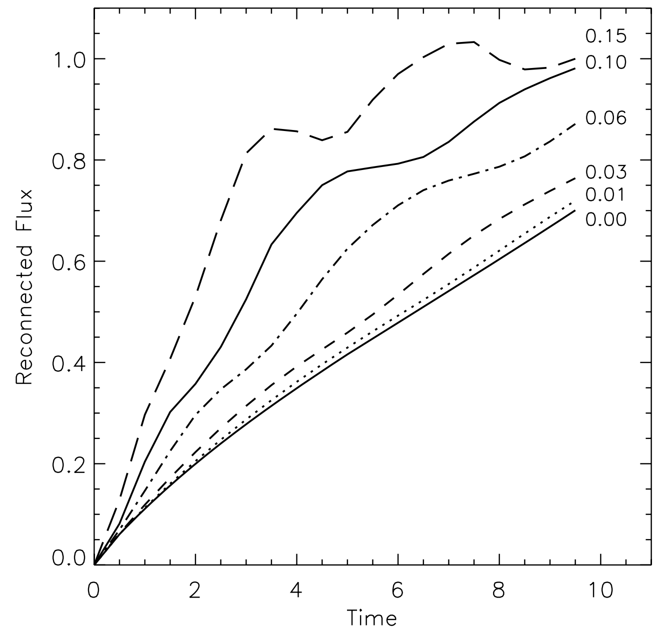

Fig. 4. Total reconnected magnetic flux as a function of time, for various simulations performed with 128^2 grid points. To the right of each curve, the corresponding value of ϵ is indicated.

One of the most important features to evaluate the efficiency of the reconnection process is the reconnected flux. The magnetic flux reconnected as a function of time at the X-point can be calculated in terms of the difference of the magnetic potential in the X-point and the O-point, i.e., $a_X(t) - a_O(t)$. The effect of the Hall term on the reconnected flux is shown in Fig. 4. As ϵ is increased the reconnection process is observed to become more efficient, as evidenced by the total reconnected flux.

5. Conclusions

We have investigated the role of the Hall effect in the magnetic reconnection process. With this goal in mind, we performed numerical simulations of the Hall MHD equations in $2\frac{1}{2}$D.

The inclusion of the Hall term leads to smaller and thinner current sheets, to the development of a quadrupolar structure in the out-of-plane magnetic field component, and to the generation of out-of-plane flows in the surroundings of the X-points.

Also, the Hall effect leads to a faster reconnection process, as evidenced by the larger total reconnected flux. From numerical simulations, an empirical scaling was obtained by Fitzpatrick (2004a) (see also Fitzpatrick (2004b)) and also by Smith et al. (2004). These studies report that the maximum reconnection rate scales like $R_{max} \approx \epsilon^{3/2}$, and that it is also sensitive to the amplitude of magnetic fluctuations. On the other hand, Wang et al. (2001) analytically derived the scaling $R_{max} \approx \epsilon^{1/2}$, which they also tested with Hall-MHD simulations. We need to run simulations at higher Reynolds numbers to test these scalings. Our current results lie in between these two predictions, but these are only preliminary conclusions because of the non-negligible role of dissipation. Note that both Fitzpatrick (2004b) and Smith et al. (2004) apply hyper-resistivity in their simulations, while we only rely on plain resistivity to break the magnetic field lines.

Acknowledgements

This work was supported by the Argentinean Grants UBACyT X209 & X329, CONICET PIP 2693, and PICTS 12187 & 14163 (ANPCyT). S.D. and D.O.G. are members of the Carrera del Investigador Científico, CONICET.

References

Birn, J., Hesse, M. J. Geophys. Res. 101, 15345–15358, 1996.
Birn, J., et al. J. Geophys. Res. 106, 3715–3719, 2001.
Canuto, C., Hussaini, M.Y., Quarteroni, A., Zang, T.A. Spectral Methods in Fluid Dynamics. Springer, New York, 1988.
Chacón, L., Knoll, D.A., Finn, J.M. Phys. Lett. A 308, 187–197, 2003.
Craig, I.J.D., Watson, P.G. Solar Phys. 214, 131–150, 2003.
Craig, I.J.D., et al. Phys. Plasmas 10, 3120–3130, 2003.
Dorelli, J.C., Phys. Plasmas 10, 3310–3314, 2003.
Dorelli, J.C., Birn, J. J. Geophys. Res. 108, 1133, 2003.
Farrugia, C.J. et al. Adv. Space Res. 28, 759, 2001.
Fitzpatrick, R., Phys. Plasmas 11, 937, 2004a.
Fitzpatrick, R., Phys. Plasmas 11, 3961, 2004b.
Gosling, J.T., et al. Geophys. Res. Lett. 22, 869, 1995.
Ma, Z., Bhattacharjee, A. Geophys. Res. 106, 3773, 2001.
Minnini, P., Gomez, D.O., Mahajan, S.M. Astrophys. J. 584, 1120, 2003.
Mozer, F., Bale, S., Phan, T.D. Phys. Rev. Lett. 89, 015002, 2002.
Parker, E.N.J. Geophys. Res. 62, 509, 1957.
Petschek, H.E. In: Ness, W.N. (Ed.), AAS/NASA Symposium on the Physics of Solar Flares. NASA, Washington, DC, p. 425, 1964.
Priest, E.R. In: Hones, E.W. (Ed.), Magnetic Reconnection in Space and Laboratory Plasmas, Geophys. Monogr. Ser., vol. 30. AGU, Washington, DC, p. 63, 1984.
Schmidt, J.M., Cargill, P.J. J. Geophys. Res. 108 (A1), 1023, doi:10.1029/2992JA009325, 2003.
Smith, D., Ghosh, S., Dmitruk, P., Matthaeus, W.H. Geophys. Res. Lett. 31, L02805, 2004.
Sonnerup, B.U.O. In: Lanzerotti, L.J., Kennel, C.F., Parker, E.N. (Eds.). New York, North-Holland, 1979.
Sonnerup, B.U.O., et al. J. Geophys. Res. 86, 10049, 1981.
Terasawa, T. Geophys. Res. Lett. 10, 475, 1984.
Wang, X., Bhattacharjee, A., Ma, Z.W. Phys. Rev. Lett. 87, 265003, 2001.